Theor Chem Acc (2009) 124:331–338
DOI 10.1007/s00214-009-0613-1

REGULAR ARTICLE

Substituent effects in the tuning of excited-state intramolecular proton transfer and optical properties of the derivatives of 2-(2-hydroxyphenyl)-5-phenyl-1,3,4-oxadiazole

Ruifa Jin · Jingping Zhang

Received: 19 May 2009 / Accepted: 15 July 2009 / Published online: 31 July 2009
© Springer-Verlag 2009

Abstract The intramolecular proton transfer process and optical properties of a series of derivatives of 2-(2-hydroxyphenyl)-5-phenyl-1,3,4-oxadiazole (HOXD) have been studied. The effects of electron-donating and -withdrawing substituents on the intramolecular proton transfer and optical properties in the S_0 and S_1 states have been investigated to find out the relationships between them and the Hammett substituent constants (δ_p). The statistically valid linear correlations are observed between the δ_p and the ionization potential (*IP*), electron affinity (*EA*), the relative energies (ΔE) and the direct energy barriers (ΔE_d) of the intramolecular proton transfer reactions, and the optical properties of HOXD and its substituted derivatives. The λ_{abs}, λ_{fl}, and λ_{ph} of the electron-withdrawing substituted derivatives have bathochromic shifts, while the corresponding values of the electron-donating substituted derivatives show hypsochromic shifts compared with the parent compound HOXD. A successful tuning in the emission color was achieved: the emission wavelength was substituent δ_p dependent, providing a powerful strategy for predicting the optical properties of novel electroluminophores.

Keywords Excited-state intramolecular proton transfer (ESIPT) · Substituent effects · UV–Vis and fluorescence spectra · 2-(2-Hydroxyphenyl)-5-phenyl-1,3,4-oxadiazole (HOXD)

1 Introduction

The excited-state intramolecular proton transfer (ESIPT) phenomenon has provoked massive interest [1–13] to the photophysicists and photochemists because of the huge potential in it since the studies of the fluorescence of methyl salicylate. ESIPT usually occurs in molecules with functional groups linked by a hydrogen bond; the charge redistribution consequent upon excitation alters the acid–base properties of these groups, leading to proton transfer along the hydrogen bond in a tautomerization process. The ESIPT process is normally extremely fast occurring within the subpicosecond time scale which falls within the range of the period of low-frequency vibrations [14]. Organic luminophores that undergo ESIPT are usually characterized by abnormally large fluorescence Stokes shifts (6,000–12,000 cm^{-1}) resulted from the reorganization of the charge distribution of the tautomerization [15, 16]. This property makes these molecules very attractive due to potential utilities in fluorescence sensors [17–19], laser dyes, organic light emitting diodes (OLEDs) [20–23], UV filters [24], and molecular switches [25, 26].

2-(2-Hydroxyphenyl)-5-phenyl-1,3,4-oxadiazole (HOXD) is an example of a molecular system that undergoes ESIPT to yield an excited keto form from the original enol form and emits quite strong ESIPT fluorescence [20, 23]. The schematic singlet and triplet potential curves in Fig. 1 describe the luminescence and protons transfers processes in HOXD (R = H) and its derivatives. The derivatives of

Electronic supplementary material The online version of this article (doi:10.1007/s00214-009-0613-1) contains supplementary material, which is available to authorized users.

R. Jin · J. Zhang (✉)
Faculty of Chemistry, Northeast Normal University, Changchun 130024, China
e-mail: zhangjingping66@yahoo.com.cn

R. Jin
Department of Chemistry, Chifeng University, Chifeng 024000, China

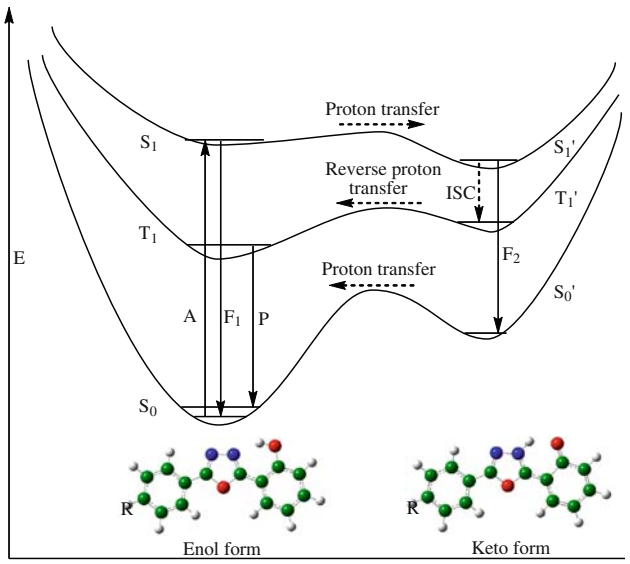

Fig. 1 Proton transfer and luminescence processes in HOXD and its derivatives. *A*, F_1, and *P* denotes the absorption, fluorescence, and phosphorescence spectra of Enol forms, respectively. F_2 denotes the fluorescence spectra of Keto forms

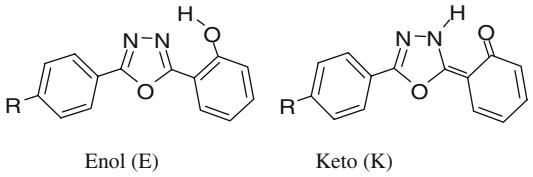

Scheme 1 Geometries of Enol (E) and Keto (K) forms of HOXD and its derivatives, along with the δ_p values of substituents (in parenthesis)

HOXD are ideal model compounds for studying the effects of substituents on the luminescent and ESIPT reaction characteristics, because the proton-donor and -acceptor parts are clearly separated [27–29]. Moreover, the triplet phosphorescence emission of the enol forms [20, 23] raises the electroluminescent efficiency that is demanding for electroluminescence materials of OLEDs in flat panel display technologies. Furthermore, substances containing an oxadiazole fragment (both low molecular weight and polymers) are promising materials for the constructing of OLEDs [30], both as electron-transporting and hole-blocking layers [31–33] and as light-emission layers [34, 35].

Experimental and theoretical studies of HOXD and its several derivatives by Doroshenko et al. [27, 28] revealed that the fluorescence properties can be tuned from a complete quenching of the phototautomer emission up to a considerable quantum yield with the introduction of electron-donating substituents either in the proton-donating or in the proton-donor moieties. Gaenko et al. [29] studied the relative effect of substituents with different electron-donor capabilities on the proton-acceptor moiety of HOXD at the high-quality level. In our previous report [36], we performed a theoretical study on O/"NH"- and O/"S"-substituted derivatives of the HOXD to investigate the substituent effects on the intramolecular protons transfer processes, the rotational processes, and the optical properties.

There have been many reports on the effects of the skeleton and the substituent groups of molecules on the luminescent and ESIPT reaction characteristics, yet general relationships between the luminescent and ESIPT reaction characteristics and the chemical structure have hitherto not been revealed. Clarification of the relationships between the chemical structure and the luminescent and ESIPT characteristics are of great value in chemistry (e.g., molecular materials, probes, sensors, and tracers) and materials science (e.g., optoelectronics), since such relationships allow us to design novel OLEDs and sensors molecular materials with ESIPT and high electroluminescent efficiency characters.

In this work, we reported some results of an extensive investigation of the intramolecular proton transfer reaction and optical properties from theoretical point of view for HOXD system. To investigate the substituent effects, a series of derivatives with electron-donating or -withdrawing substituents on the phenyl ring of HOXD, as shown in Scheme 1, have been designed. The substituents are considered with the Hammett sigma para constants (δ_p) values ranging from electron donor such as –OH ($\delta_p = -0.37$) to strong electron acceptor (e.g., –CN, $\delta_p = 0.66$). We investigated the effects of electron-donating and -withdrawing substituents on the intramolecular proton transfer properties in the ground (S_0) and first singlet excited (S_1) states to find out the relationships between the ESIPT reaction properties and the δ_p. Furthermore, we explored the optical properties of the substituted derivatives at the TD-DFT level with the aim to get the relationships between the optical properties of the substituted derivatives and the δ_p.

2 Computational methods

All calculations discussed in this work are carried out by means of the GAUSSIAN 03 package [37]. On the basis of our previous successful calculation for HOXD [36], the geometry optimizations for S_0 states were performed using the ab initio Hartree Fock (HF) method, while the configuration interaction with single excitations (CIS) [38] method was employed to optimize the geometries for S_1 and T_1 states. All geometry optimizations were performed

using the 6-31G(d) basis set. Frequency calculations at the same level were performed for the obtained structures. All real frequencies have confirmed the presence of a local minimum, while one imaginary frequency indicated the existence of a transition state.

To introduce the dynamic electron correlation, single-point energy calculations for the ground and excited states have been done at the DFT and TD-DFT [39–41] level, respectively, with B3LYP, Becke's three-parameter functional, and with nonlocal correlation provided by the LYP [42] expression, using the 6-31+G(d,p) basis set. Absorption, fluorescence, and phosphorescence spectra were calculated at the TD-B3LYP/6-31+G(d,p) level based on the optimized geometries in S_0, S_1, and T_1 states, respectively, which has been proved to be efficient in providing proper optical properties [43–46]. The radiative rate constants were also calculated. The hybrid method (denoting as single point calculation//optimization method) such as DFT//HF or TD-DFT//HF or TD-DFT//CIS has been proved to be an efficient approach in predicting energy parameters [47, 48] or optical properties for LED materials [43–46, 49–54].

In our previous work [36], the geometry optimizations for the excited state of HOXD were also carried out at the TD-B3LYP/TZVP level by TURBOMOLE 5.7 [55] program suite. The optical properties were predicted at the TD-B3LYP/TZVP level based on the optimized excited states geometries. Our results revealed that the TD-B3LYP/TZVP method failed to provide a correct energy ordering with the available experimental result for the T_1 state. It was also found that TD-DFT method systematically underestimates the energy of charge transfer excited states [56]. To the contrary, the TD-B3LYP/6-31+G(d,p)//CIS/6-31G(d) method provided a correct energy ordering with the available experimental result for the excited states (S_1 and T_1). Furthermore, the TD-B3LYP/6-31+G(d,p)//CIS/6-31G(d) method performs better in predicting the λ_{fl} and λ_{ph} for HOXD compared with the experimental data. Hence, in this work, we perform the geometry optimizations for the excited states of HOXD and its substituted derivatives at the CIS/6-31G(d) level.

The ionization potential (*IP*) and electron affinity (*EA*) for the Enol (^{1}E) forms of HOXD and its substituted derivatives were calculated as described in the following equations:

$$IP = E(M^+) - E(M^0)$$
$$EA = E(M^0) - E(M^-)$$

where the $E(M^0)$, $E(M^+)$, and $E(M^-)$ are the total energy of the neutral, cationic, and anionic forms of HOXD and its substituted derivatives at the B3LYP/6-31+G(d,p) level, respectively.

3 Results and discussion

3.1 Substituent effects on the electronic structures and properties of the substituted derivatives

To investigate the effects of different substituents on the phenyl ring of HOXD on the electronic structures and properties of the substituted derivatives, a diverse set of 15 substituted HOXDs have been considered. The properties of the different electron donors or acceptors can be nicely summarized in terms of the δ_p [57], one of the most widely used means for the study and interpretation of reactions mechanisms and properties of organic compounds [58–68]. A positive value of δ_p indicates that the substituent group is electron-withdrawing in nature; on the other hand, a negative value implies the electron-donating nature of the substituent. The δ_p values are taken from the compilations of the δ_p by Hansch and Taft [58]. All the calculations were made for the molecules in gas phase. It is worth to note that the experimental δ_p values were obtained initially in polar solutions, which perhaps causes the systematic deviations for the data points corresponding to substituents. However, statistically valid linear correlations at least can be observed between the electronic structures and/or properties and their δ_p.

The introduction of different electron-donating or -withdrawing groups for the parent compound HOXD leads to the change of the electronic structures and properties for its derivatives. The *IP* and *EA* are important properties for organic dyes used in OLEDs, and the light emitting materials should have a small *IP* and large *EA* [30, 31, 69].

The *IP* and *EA* values of HOXD derivatives are plotted as a function of the δ_p in Fig. 2. The *IP* and *EA* of the ^{1}E

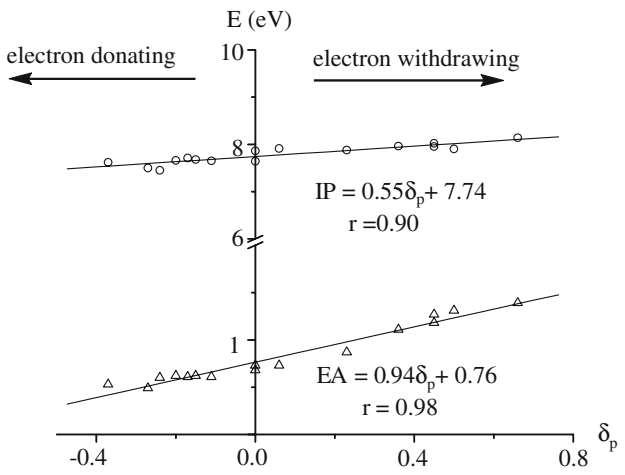

Fig. 2 Ionization potential (*IP*) and electron affinity (*EA*) versus δ_p for HOXD and its substituted derivatives at the B3LYP/6-31+G(d,p) level

forms for HOXD and its substituted derivatives are collected in supplementary Table SI. The results displayed in Fig. 2 reveal that the linear correlations (correlation coefficient: $r = 0.90$ and 0.98; slope: $\rho = 0.55$ and 0.94 for *IP* and *EA*, respectively) are observed between the *IP*/*EA* and δ_p, indicating that the trend in the substituent effects can be qualitatively understood in terms of the electron-donating or -withdrawing character of the substituents. One can also find that both the *IP* and *EA* increase with the increasing electron-withdrawing abilities of the substituent (i.e., higher value for δ_p). The *IP* and *EA* of electron-withdrawing (-donating) substituted derivatives are larger (smaller) than those of HOXD. It suggests that the electron-donating (-withdrawing) groups favor the decrease (increase) for the *IP* and *EA*. Furthermore, the comparison of line slopes indicates that groups exert stronger influence upon *EA* than *IP*, i.e., the increase in *EA* with δ_p is significantly steeper than that of *IP*.

3.2 Substituent effects on the intramolecular proton transfer reaction properties of the substituted derivatives in S_0, S_1, and T_1 states

The relative energies (ΔE) (energies differences between products and reactants), the direct (ΔE_d), and reverse (ΔE_r) energy barriers for the protons transfer of $^1K \rightarrow {}^1E$ in S_0 states and $^1E^* \rightarrow {}^1K^*$ in S_1 states of HOXD and its substituted derivatives are summarized in supplementary Table SII. The ΔE, ΔE_d, and ΔE_r in S_0 and S_1 states are plotted in Fig. 3a and b as a function of δ_p, respectively. For the strongest electron-donating groups, *p*-NMe_2 and *p*-NH_2 ($\delta_p = -0.83$ and -0.66), their estimated rate constants of the ESIPT reactions are very small and the protons transfer reactions are very slow [27, 29]. So, we exclude them from this system.

Inspection of Fig. 3a reveals clearly that ^1E forms are much more stable than ^1K forms ($\Delta E < -0.58$ eV), indicating that both electron-withdrawing and -donating substituents stabilize the ^1E forms relative to their ^1K forms. Moreover, the line slopes of ΔE, ΔE_d, and ΔE_r are only -0.044, -0.0064, and 0.037 eV/mol, respectively, suggesting that the substituent effects do not significantly affect the ΔE, ΔE_r, especially for ΔE_d compared with those of HOXD. Therefore, the protons transfer processes $^1K \rightarrow {}^1E$ of both electron-withdrawing and -donating substituted derivatives can take place easily though low energy barriers or barrierless processes. To the contrary, the reverse protons transfer processes in S_0 states are difficult to occur for both electron-withdrawing and -donating substituted derivatives as HOXD. Following trend is observable from Fig. 3a: both ΔE and ΔE_d slightly decrease while ΔE_r slightly increase with the increasing electron-withdrawing abilities of the substituents, indicating that the high electron-withdrawing (-donating) abilities of the substituents slightly increase (decrease) the stabilities of ^1E forms compared with their ^1K forms; furthermore, the protons transfer processes in S_0 states involve high ΔE_r and slightly negative values of ΔE_d. The slightly negative values of ΔE_d suggest that the B3LYP method slightly underestimates the energy barriers of the protons transfer processes. It was also recently reported that the B3LYP method provides negative energy barriers for radical addition reaction [70].

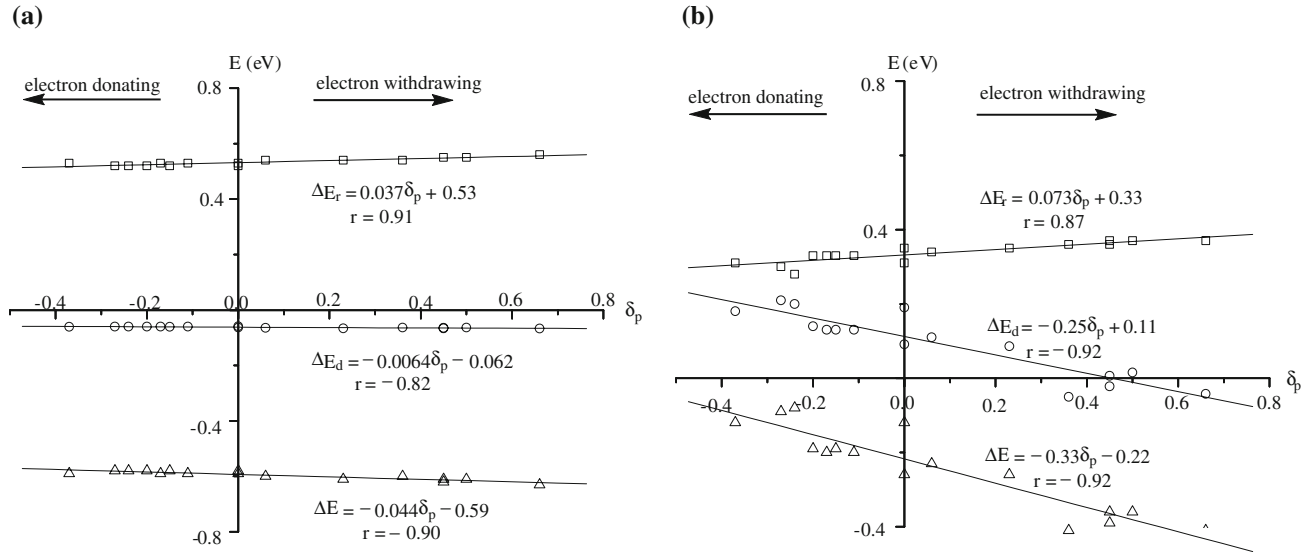

Fig. 3 The interaction energies (ΔE), direct (ΔE_d), and reverse (ΔE_r) energy barriers for the intramolecular protons transfer processes of HOXD and its substituted derivatives versus δ_p (**a**) in S_0 state at the B3LYP/6-31+G(d,p)//HF/6-31G(d) level and (**b**) in S_1 state at the TD-B3LYP/6-31+G(d,p)//CIS/6-31G(d) level

Therefore, the large endothermicity and high ΔE_r impose a restriction on the occurrence of the reverse protons transfer processes $^1E \rightarrow {}^1K$ in S_0 states for all compounds. However, the protons transfer processes will occur easily through a very low energy barriers or barrierless processes.

Comparing the results shown in Fig. 3a with 3b, one can find that the introduction of different electron-donating or -withdrawing group to the HOXD leads to similar trends of the ΔE, ΔE_d, and ΔE_r in S_1 states compared with those in S_0 states. A careful inspection of the results displayed in Fig. 3a and b confirms the expectation. Both ΔE and ΔE_d linearly decrease substantially with the increase of electron-withdrawing abilities of the substituents compared with those in S_0 state with the line slopes of -0.33 and -0.25 eV/mol, respectively. The ΔE_r in S_1 states slightly increase with the increase of electron-withdrawing abilities of the substituents as those in S_0 states with the line slope of 0.073 eV/mol. The dependences of ΔE and ΔE_d on substitutions in S_1 states are remarkably more significant than those of ΔE_r. Therefore, by substituting electron-withdrawing (-donating) groups, the ΔE and ΔE_d decrease (increase) and the ΔE_r increase (decrease) in S_1 states, compared with those of HOXD, respectively.

The endothermic reverse protons transfer processes $^1E \rightarrow {}^1K$ of all derivatives in S_0 states become exothermic ESIPT processes $^1E^* \rightarrow {}^1K^*$ in S_1 states ($\Delta E < 0$). The reverses of the stabilities of the $^1E^*$ and $^1K^*$ forms are found because of the loss of aromaticity in the excitation processes, which favor the ESIPT reactions. One can find that the ΔE values of electron-withdrawing substituted derivatives in S_1 states are more negative than those of electron-donating substituted derivatives (Fig. 3b). This indicates that the stabilizing effects of the electron-withdrawing substituents on the $^1K^*$ forms are stronger than those of electron-donating substituents compared with their $^1E^*$ forms. Therefore, the stabilities of $^1K^*$ forms increase by strong electron-withdrawing groups and decrease by strong electron-donating groups compared with their $^1E^*$ forms, respectively.

Comparing the ΔE_d in S_1 states and the ΔE_r in S_0 states shown in Fig. 3a and b, the ΔE_d in S_1 states decrease substantially while the ΔE_r in S_0 states increase slightly with the increasing electron-withdrawing abilities of the substituents. The line slopes of the ΔE_d in S_1 states and the ΔE_r in S_0 states are -0.25 and 0.037 eV/mol, respectively. Thus, each ESIPT process of all derivatives can take place easily through an exothermic process and a lower energy barrier. Moreover, the ESIPT processes of the electron-withdrawing substituted derivatives take place more easily than those of the electron-donating substituted derivatives through the very low energy barriers. However, the reverse ESIPT processes of the electron-withdrawing substituted derivatives will occur more difficultly than those of the electron-donating substituted derivatives.

3.3 Substituent effects on the absorption, fluorescence, and phosphorescence spectra of the substituted derivatives

The schematic singlet and triplet potential curves describe the luminescence and proton-transfer processes in HOXD and its derivatives, as shown in Fig. 1. Initially, the molecules are in the ^1E forms in S_0 states. Upon photoexcitation, ESIPT occurs, the protons transfer from $^1E^*$ to $^1K^*$ forms in S_1 states. Later, the $^1K^*$ return from S_1 to S_0 states ($^1K^* \rightarrow {}^1K$) through fluorescent emissions. Finally, the protons transfer from ^1K to the starting ^1E in thermal processes in S_0 states to finish the cyclic four-level photophysical scheme ($^1E \rightarrow {}^1E^* \rightarrow {}^1K^* \rightarrow {}^1K \rightarrow {}^1E$). Furthermore, the $^1K^*$ can also transit to the excited triplet states of the keto forms ($^3K^*$) through the intersystem crossing (ISC). For molecules with ESIPT property, it was found that the ESIPT facilitates the ISC [71]. Subsequently, if enol forms ($^3E^*$) are more stable than $^3K^*$ forms, $^3K^*$ forms will take place the reverse protons transfer in T_1 states to form $^3E^*$ forms. Eventually, phosphorescences of $^3E^*$ forms will be observed ($^1K^* \rightarrow {}^3K^* \rightarrow {}^3E^* \rightarrow {}^1E$) [71].

The absorption corresponds to the excitation of ^1E forms from S_0 to S_1 states. So the λ_{abs} are calculated at the TD-B3LYP/6-31+G(d,p) level based on the optimized geometries of ^1E forms in S_0 states. The fluorescent emission bands characterized by high Stocks shift values are attributed to the emissions of $^1K^*$ forms formed by ESIPT. The phosphorescence emission bands are attributed to the emissions of $^3E^*$ forms because all the $^3E^*$ forms of HOXD and its derivatives are more stable than their $^3K^*$ forms. Therefore, the λ_{fl} and λ_{ph} are calculated at the TD-B3LYP/6-31+G(d,p) level based on the optimized geometries of $^1K^*$ and $^3E^*$ forms in S_1 and T_1 states, respectively.

It is well known that solvent effects differently tune the absorption and emission wavelengths. We select HOXD and the derivatives with strongest electron-donating and -withdrawing substituents (e.g., –OH and –CN, $\delta_p = -0.37$ and 0.66) in this study to investigate the solvent effect for optical properties of this kind of compounds using the polarized continuum model (PCM) [72]. On the basis of the optimized structures (S_0, S_1, and T_1), we predicted the optical spectra for HOXD and its derivatives (R = CN and OH) in CH_2Cl_2 solvent taking into account both nonequilibrium and equilibrium solute-solvent effects [73] at the PCMTD-B3LYP/6-31+G(d,P) level. The calculated maximum wavelength λ_{abs}, λ_{fl}, and λ_{ph} in nonequilibrium and equilibrium solvations in CH_2Cl_2 solvent are listed in supplementary Table SIII. The results displayed in Table SIII show that the introduction of the solvent effects in the TD-DFT calculations does not significantly affect the λ_{abs} values. The deviations of λ_{abs} in CH_2Cl_2 and in gas phase

are <4 nm in nonequilibrium solvation, the corresponding deviations in equilibrium solvation are estimated to be 2–10 nm, the difference between nonequilibrium and equilibrium results being <6 nm. The λ_{ph} values of HOXD and the derivative with strongest electron-donating group (R = OH) in CH_2Cl_2 taking into account of both nonequilibrium and equilibrium solute-solvent effects have hypsochromic shifts (11 and 55 nm), while the corresponding value of the derivative with strongest electron-withdrawing substituent (R = CN) shows bathochromic shift (35 nm) compared with the λ_{ph} values in gas phase. To the contrary, the λ_{fl} values of HOXD and its derivatives in CH_2Cl_2 taking into account of solvent effects show high hypsochromic shifts, which are estimated to be 8–75 nm in nonequilibrium salvation and 14–67 nm in equilibrium salvation, respectively, compared with the values in gas phase, particularly the highest hypsochromic shift is observed for the derivative with strongest electron-withdrawing substituent (R = CN). Inspection of Table SIII reveals clearly that high electron-withdrawing (electron-donating) ability of the substituent increases (decreases) the hypsochromic shifts of λ_{fl} value compared with its λ_{fl} value in gas phase. Nevertheless, the introduction of the solvent effect in the TD-DFT calculation leads to larger deviation of λ_{fl} for HOXD from the experimental data [18]. As PCM calculation is very time consuming for such large molecule, hereafter, we will not consider the solvent effects in the TD-DFT calculations.

The calculated absorption (λ_{abs}), fluorescence (λ_{fl}), and phosphorescence (λ_{ph}) spectra at the TD-B3LYP/6-31+G(d,p) level based on the HF/6-31G(d) (for λ_{abs}) and CIS/6-31G(d) (for λ_{fl} and λ_{ph}) optimized geometries are summarized in supplementary Table SIV. The λ_{abs}, λ_{fl}, and λ_{ph} are plotted as a function of δ_p, as shown in Fig. 4. The

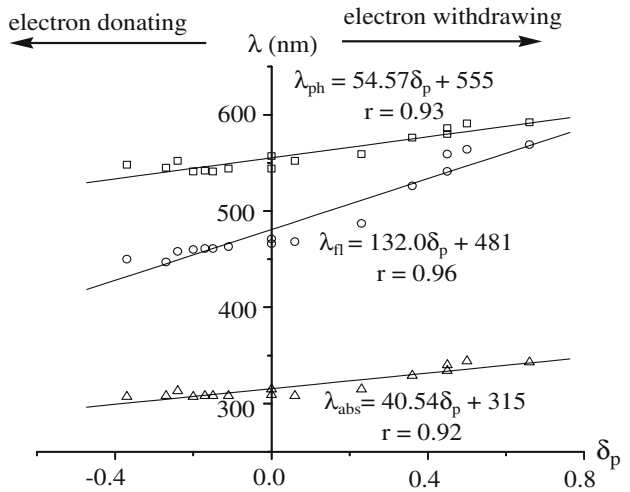

Fig. 4 Maximum absorption (λ_{abs}) of ^{1}E forms, fluorescence (λ_{fl}) of ^{1}K* forms, and phosphorescence (λ_{ph}) of ^{3}E* forms for HOXD and its substituted derivatives versus δ_p at the TD-B3LYP/6-31+G(d,p) level

results are worth noting that the λ_{abs}, λ_{fl}, and λ_{ph} linearly increase with the increase of the electron-withdrawing abilities of substituents. All the λ_{abs}, λ_{fl}, and λ_{ph} of the electron-withdrawing substituted derivatives have bathochromic shifts, while the corresponding values of the electron-donating substituted derivatives show hypsochromic shifts compared with those of HOXD. Furthermore, all the line slopes of λ_{abs}, λ_{fl}, and λ_{ph} are positive, indicating high electron-withdrawing ability of the substituents increase the bathochromic shifts values of λ_{abs}, λ_{fl}, and λ_{ph} for the electron-withdrawing substituted derivatives, while high electron-donating ability of the substituents increase the hypsochromic shifts values of λ_{abs}, λ_{fl}, and λ_{ph} for the electron-donating substituted derivatives compared with those of HOXD.

The line slopes of λ_{abs}, λ_{fl}, and λ_{ph} are 40.54, 132.0, and 54.57 nm, respectively. The line slope of λ_{ph} is higher by 14 nm than that of λ_{abs}, indicating that the substituent effects on the λ_{ph} are stronger than those on the λ_{abs}. The line slope of λ_{fl} (132.0 nm) is higher by 91 and 77 nm than those of λ_{abs} and λ_{ph}, respectively. The comparison of line slopes indicates that substituent effects exert stronger influence upon λ_{fl} than λ_{abs} and λ_{ph}, i.e., the increase in λ_{fl} with the increasing δ_p is significantly steeper than those of λ_{abs} and λ_{ph}, respectively. Hence, the sensitivities of the λ_{fl} to substitutions are significantly higher than those of the λ_{abs} and λ_{ph}, respectively. Thus, a powerful tuning in the absorptions and emissions can be achieved: the absorptions and emissions wavelengths are the δ_p of the substituents dependent, providing a powerful strategy for prediction of the optical properties of novel electroluminophores.

Especially, it is very interesting that the line intercepts of λ_{abs} and λ_{fl} (i.e., pristine HOXD for $\delta_p = 0$) are 315 and 481 nm, respectively. The results are both in excellent agreement with experimental results (315 and 475 nm, respectively) [18], with the maximum deviation being <6 nm. The line intercept of λ_{ph} (555 nm) is in good agreement with the calculated data (543 nm) in [36], although there is a larger deviation of λ_{ph} from the experimental data (481 nm) [18].

The substantial effects of the substitutions pattern on the optoelectronic properties of substituted derivatives of HOXD prompted us to rationalize the data in terms of a Hammett-type linear radiative rate constants k_f and natural radiative lifetimes τ_r relationship. We utilize Einstein's spontaneous emission transition probability relation [27, 29, 74, 75]:

$$k_f = \frac{fv^2}{1.5}$$

where k_f is the radiative rate constant (in s^{-1}), v is the transition wavenumber (in cm^{-1}), and f is the corresponding oscillator strength. The inverse of k_f yields the

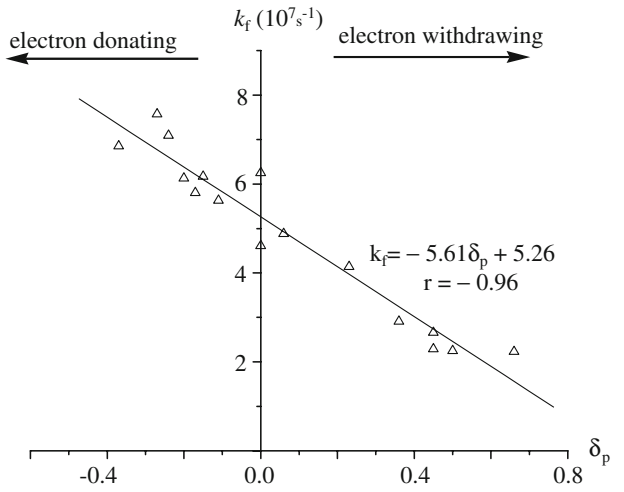

Fig. 5 Radiative rate constants (k_f) of HOXD and its substituted derivatives versus δ_p in S_1 state at the TD-B3LYP/6-31+G(d,p)//CIS/6-31G(d) level

natural radiative lifetime, τ_r [76]. The k_f and τ_r of HOXD and its derivatives are summarized in supplementary Table SV.

The values of k_f are plotted in Fig. 5 as a function of the δ_p. The τ_r versus δ_p is shown in supplementary Fig. SI. A linear correlation ($r = -0.96$) is observed between k_f and the δ_p. The electron-donating (-withdrawing) substituents cause increase (decrease) in substituted derivative's k_f compared with that of HOXD. The electron-donating substituents cause decrease in substituted derivative's τ_r, whereas electron-withdrawing groups increase τ_r compared with that of HOXD. Hence, the Hammett analysis provides a valuable tool to predict the k_f and τ_r of substituted derivatives.

4 Conclusions

The statistically valid linear correlations are observed between the *IP*, *EA*, the ΔE, ΔE_d, and ΔE_r of the protons transfer processes, and the λ_{abs}, λ_{fl}, and λ_{ph} of HOXD and its substituted derivatives and the δ_p. The following conclusions can be drawn. (1) The linear correlations are observed between the *IP* and *EA* of the substituted derivatives and the δ_p, indicating that the trend in the substituent effects can be qualitatively understood in terms of the electron-donating or -withdrawing character of the substituents. (2) For the protons transfer reactions, the substituent effect has little effect on the ΔE, ΔE_d, and ΔE_r of $^1K \rightarrow {}^1E$ compared with those of HOXD in S_0 states. The reverse protons transfer processes in S_0 states are difficult to occur for both electron-withdrawing and -donating substituted derivatives as HOXD. To the contrary, the protons transfer processes of both electron-withdrawing and -donating substituted derivatives can take place easily though low energy barriers or barrierless processes. In S_1 states, both the ΔE and ΔE_d linearly decrease substantially, while the ΔE_r increase with the increasing electron-withdrawing ability of the substituents for ESIPT processes of $^1E^* \rightarrow {}^1K^*$ compared with those of HOXD. Therefore, the ESIPT processes of the electron-withdrawing substituted derivatives occur more easily than those of the electron-donating substituted derivatives through very low energy barriers. To the contrary, the reverse ESIPT processes of the electron-withdrawing substituted derivatives will occur more difficultly than those of the electron-donating substituted derivatives. (3) The λ_{abs}, λ_{fl}, and λ_{ph} of the electron-withdrawing substituted derivatives have bathochromic shifts, while the corresponding values of the electron-donating substituted derivatives show hypsochromic shifts compared with those of HOXD. Furthermore, the substituent effect on the λ_{fl} is stronger than those of λ_{abs} and λ_{ph}, respectively. (4) A correlation is found for substituted derivatives between k_f and τ_r and the δ_p of substituted derivatives. The emission color can be tuned by substituents, providing a powerful strategy for prediction of the optical properties of novel electroluminophores.

Acknowledgments Financial supports from the NSFC (Nos. 50873020, 20773022), the NCET-06-0321, and the NENU-STB-07-007 are gratefully acknowledged.

References

1. Chen C-L, Lin C-W, Hsieh C-C, Lai C-H, Lee G-H, Wang C-C, Chou P-T (2009) J Phys Chem A 113:205
2. Park S, Seo J, Kim SH, Park SY (2008) Adv Funct Mater 18:726
3. Nosenko Y, Wiosna-Sałyga G, Kunitski M, Petkova I, Singh A, Buma WJ, Thummel RP, Brutschy B, Waluk J (2008) Angew Chem Int Ed Engl 47:6037
4. Migani A, Bearpark MJ, Olivucci M, Robb MA (2007) J Am Chem Soc 129:3703
5. Shynkar VV, Klymchenko AS, Kunzelmann C, Duportail G, Muller CD, Demchenko AP, Freyssinet J-M, Mely Y (2007) J Am Chem Soc 129:2187
6. Wu Y, Peng X, Fan J, Gao S, Tian M, Zhao J, Sun S (2007) J Org Chem 72:62
7. Henary MM, Wu Y, Cody J, Sumalekshmy S, Li J, Mandal S, Fahrni CJ (2007) J Org Chem 72:4784
8. Qian Y, Li S, Zhang G, Wang Q, Wang S, Xu H, Li C, Li Y, Yang G (2007) J Phys Chem B 111:5861
9. Sakota K, Inoue N, Komoto Y, Sekiya H (2007) J Phys Chem A 111:4596
10. Strandjord AJG, Courtney SH, Friedrich DM, Barbara PF (1983) J Phys Chem 87:1125
11. McMorrow D, Kasha M (1984) J Phys Chem 88:2235
12. Schwartz BJ, Peteanu LA, Harris CB (1992) J Phys Chem 96:3591
13. Sengupta PK, Kasha M (1979) Chem Phys Lett 68:382
14. Das K, Sarkar N, Ghosh AK, Majumdar D, Nath DN, Bhattacharyya K (1994) J Phys Chem 98:9126

15. Douhal A, Lahmani F, Zewail AH (1996) Chem Phys 207:477
16. Douhal A, Lahmani F, Zehnacker-Rentien A (1993) Chem Phys 178:493
17. Sytnik A, Kasha M (1994) Proc Natl Acad Sci USA 91:8627
18. Liang F, Wang L, Ma D, Jing X, Wang F (2002) Appl Phys Lett 81:4
19. Tong H, Zhou G, Wang L, Jing X, Wang F, Zhang J (2003) Tetrahedron Lett 44:131
20. Brunner K, Dijken AV, Börner H, Bastiaansen JJAM, Kiggen NMM, Langeveld BMW (2004) J Am Chem Soc 126:6035
21. Yi Y, Zhu L, Shuai Z (2008) Macromol Theory Simul 17:12
22. Parthenopoulos DA, McMorrow D, Kasha M (1991) J Phys Chem 95:2668
23. Ma D, Liang F, Wang L, Lee ST, Hung L (2002) Chem Phys Lett 358:24
24. Keck J, Kramer HEA, Port H, Hirsch T, Fischer P, Rytz G (1996) J Phys Chem 100:14468
25. Douhal A, Sastre R (1994) Chem Phys Lett 219:91
26. Photochromism: memories and switches (2000) Special issue of Chem Rev 100
27. Doroshenko AO, Posokhov EA, Verezubova AA, Ptyagina LM (2000) J Phys Org Chem 13:253
28. Doroshenko AO, Posokhov EA, Verezubova AA, Ptyagina LM, Skripkina VT, Shershukov VM (2002) Photochem Photobiol Sci 1:92
29. Gaenko AV, Devarajan A, Tselinskii IV, Ryde U (2006) J Phys Chem A 110:7935
30. Tamoto N, Adachi C, Nagai K (1997) Chem Mater 9:1077
31. Uchida M, Adachi C, Koyama T, Taniguchi Y (1999) J Appl Phys 86:1680
32. Wang JF, Jabbour GE, Mash EA, Anderson J, Zhang Y, Lee PA, Armstrong NR, Peyghambarian N, Kippelen B (1999) Adv Mater 11:1266
33. Kido J, Hayase H, Hongawa K, Nagai K, Okuyama K (1994) Appl Phys Lett 65:2124
34. Antoniadis H, Inbasekaran M, Woo EP (1998) Appl Phys Lett 73:3055
35. Hu Y, Zhang Y, Liang F, Wang L, Ma D, Jing X (2003) Synth Met 137:1123
36. Yang Z, Yang S, Zhang J (2007) J Phys Chem A 111:6354
37. Frisch MJ, Trucks GW, Schlegel HB, Scuseria GE, Robb MA, Cheeseman JR, Montgomery JAJ, Vreven T, Kudin KN, Burant JC, Millam JM, Iyengar SS, Tomasi J, Barone V, Mennucci B, Cossi M, Scalmani G, Rega N, Petersson GA, Nakatsuji H, Hada M, Ehara M, Toyota K, Fukuda R, Hasegawa J, Ishida M, Nakajima T, Honda Y, Kitao O, Nakai H, Klene M, Li X, Knox JE, Hratchian HP, Cross JB, Adamo C, Jaramillo J, Gomperts R, Stratmann RE, Yazyev O, Austin AJ, Cammi R, Pomelli C, Ochterski JW, Ayala PY, Morokuma K, Voth GA, Salvador P, Dannenberg JJ, Zakrzewski VG, Dapprich S, Daniels AD, Strain MC, Farkas O, Malick DK, Rabuck AD, Raghavachari K, Foresman JB, Ortiz JV, Cui Q, Baboul AG, Clifford S, Cioslowski J, Stefanov BB, Liu G, Liashenko A, Piskorz P, Komaromi I, Martin RL, Fox DJ, Keith T, Al-Laham MA, Peng CY, Nanayakkara A, Challacombe M, Gill PMW, Johnson B, Chen W, Wong MW, Gonzalez C, Pople JA (2004) Gaussian 03, revision C.02. Gaussian Inc, Wallingford
38. Foresman JB, Head-Gordon M, Pople JA, Frisch MJ (1992) J Phys Chem 96:135
39. Dreuw A, Head-Gordon M (2005) Chem Rev 105:4009
40. Barone V, Polimeno A (2007) Chem Soc Rev 36:1724
41. Jacquemin D, Perpete EA, Ciofini I, Adamo C (2009) Acc Chem Res 42:326
42. Lee C, Yang W, Parr RG (1988) Phys Rev B 37:785
43. Sun M, Niu B, Zhang J (2008) J Mol Struct: Theochem 862:85
44. Sun M, Niu B, Zhang J (2008) Theor Chem Acc 119:489
45. Gahungu G, Zhang J (2005) J Mol Struct: Theochem 755:19
46. Li Z, Zhang J (2006) Chem Phys 331:159
47. Domingo LR, Picher MT, Zaragozá RJ (1998) J Org Chem 63:9183
48. Shukla MK, Leszczynski J (2005) Int J Quantum Chem 105:387
49. Halls MD, Schlegel HB (2001) Chem Mater 13:2632
50. Zhang J, Frenking G (2004) J Phys Chem A 108:10296
51. Zhang J, Frenking G (2004) Chem Phys Lett 394:120
52. Gahungu G, Zhang J (2005) J Phys Chem B 109:17762
53. Gahungu G, Zhang J (2005) Chem Phys Lett 410:302
54. Hu B, Gahungu G, Zhang J (2007) J Phys Chem A 111:4965
55. Ahlrichs R, Bär M, Häser M, Horn H, Kälmel C (1989) Chem Phys Lett 162:165
56. Santos L, Vargas A, Moreno M, Manzano BR, Lluch JM, Douhal A (2004) J Phys Chem A 108:9331
57. Hammett LP (1937) J Am Chem Soc 59:96
58. Hansch C, Leo A, Taft RW (1991) Chem Rev 91:165
59. Wheeler SE, Houk KN (2008) J Am Chem Soc 130:10854
60. Romero FA, Hwang I, Boger DL (2006) J Am Chem Soc 128:14004
61. Zdilla MJ, Dexheimer JL, Abu-Omar MM (2007) J Am Chem Soc 129:11505
62. Pohl R, Anzenbacher P Jr (2003) Org Lett 5:2769
63. Pohl R, Montes VA, Shinar J, Anzenbacher P Jr (2004) J Org Chem 69:1723
64. Pan Y, Fu Y, Liu S, Yu H, Gao Y, Guo Q, Yu S (2006) J Phys Chem A 110:7316
65. Zhang X, Wang C-J, Liu L-H, Jiang Y-B (2002) J Phys Chem B 106:12432
66. Fayet G, Joubert L, Rotureau P, Adamo C (2008) J Phys Chem A 112:4054
67. Cleij TJ, King JK, Jenneskens LW (2000) Macromolecules 33:89
68. Jacquemin D, Champagne B, André J-M (1996) Synth Met 80:205
69. Sugiyama K, Yoshimura D, Miyamae T, Miyazaki T, Ishii H, Ouchi Y, Seki K (1998) J Appl Phys 83:4928
70. Jena NR, Mishra PC (2005) J Phys Chem B 109:14205
71. Kasha M, Heldt J, Gormin D (1995) J Phys Chem 99:7281
72. Cossi M, Rega N, Scalmani G, Barone V (2003) J Comput Chem 24:669
73. Cossi M, Barone V (2001) J Chem Phys 115:4708
74. Aquino AJA, Lischka H, Hattig C (2005) J Phys Chem A 109:3201
75. Joachain CJ, Brandsen BH (1983) Physics of atoms and molecules. Longman, London
76. Köse ME, Mitchell WJ, Kopidakis N, Chang CH, Shaheen SE, Kim K, Rumbles G (2007) J Am Chem Soc 129:14257